Protein Crystals

DOI: 10.1002/anie.200800151

From Native to Non-Native Two-Dimensional Protein Lattices through Underlying Hydrophilic/Hydrophobic Nanoprotrusions**

*Susana Moreno-Flores, Amal Kasry, Hans-Juergen Butt, Chandrasekhar Vavilala, Michael Schmittel, Dietmar Pum, Uwe Bernd Sleytr, and Jose Luis Toca-Herrera**

Protein crystallization is a crucial step in the study of protein structure and function,[1] as well as in biosensing.[2–4] In many cases, it proceeds under ill-controlled conditions, which make it difficult to predict the outcome or feasibility. On the other hand, controlled two-dimensional (2D) protein recrystallization has been mainly accomplished through metal-ion coordination to accessible histidine residues[5] or specific interactions with high-affinity ligands.[6] Both approaches, however, involve knowledge of the protein structure and, in some cases, protein engineering. In this work, we show that control of the morphology of a 2D wild-type protein crystal is possible by using a *chemical nanotuner* as a substrate. In this way, nonspecific substrate–protein interactions can be finely modulated to select the self-assembly pathway to the corresponding protein crystal. Our model system consists of a bacterial S-layer, a two-dimensional (glyco)protein crystal located in the cell wall of many prokaryotic organisms.[7] The S-layers act as selective, protective barriers that mediate cell development.[8] The chemical nanotuner is a set of self-assembled monolayers (SAMs) of dialkyldisulfide derivatives with the formula $CH_3(CH_2)_{11+m}SS(CH_2)_{11}OH$, in which m is the chain-length difference in methylene units between the methyl- and the hydroxy-terminated branches.[9] The resulting surface is composed of OH- and CH_3-terminated thiolates in a stand-up conformation with a defined chemical functionality ratio of 50%. These SAMs contain submolecular protrusions whose nature is controlled by the m value: $m<0$ indicates that the protruding chains are OH terminated, whereas $m>0$ denotes that the surface protrusions are methyl functionalized (Figure 1). The variation in the m value determines the protein-recrystallization route.

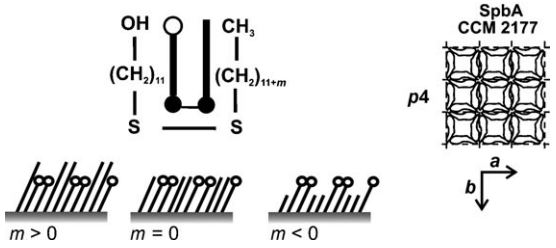

Figure 1. Disulfides, SAMs, and bacterial S-layers used in this study. The bacterial S-layers (SbpA CCM 2177) have a native *p*4 symmetry (square lattices) with unit-cell vectors *a* and *b*.

S-layers undergo a morphological transformation when recrystallized on substrates with polar- and nonpolar-terminated (nano)protrusions. In Figure 2, atomic force microscopy (AFM) images show that both crystal size and lattice parameters depend on the chemical nature and extent of the protruding groups. According to the data in Table 1 the crystal domains undergo an overall 10-fold decrease upon gradual elongation of the hydrophobic capped chain in the SAM (i.e. m varying from -6 to +6), while the lattice constants increase from 13 nm (typical values found in bacteria)[7] to 15.5 nm. Furthermore, the S-layer thickness changes from 14–15 nm (a bilayer)[10,11] down to 8 nm (a monolayer),[12,13] as indicated in Table 1.

Not only the outcome but also the process is different. Surface plasmon resonance (SPR) measurements show that S-layer formation exhibits two types of kinetics upon variation of the m value. For $m=-6$, the change in reflectivity with time undergoes a sudden increase followed by a gradual, shoulder-like increase prior to stabilization (Figure 3a, dotted

[*] Dr. S. Moreno-Flores, Dr. J. L. Toca-Herrera
Biosurfaces Dept. CIC BiomaGUNE
Paseo Miramon 182, 20009 San Sebastian (Spain)
Fax: (+34) 943-005-315
E-mail: jltocaherrera@cicbiomagune.es
Homepage: http://www.cicbiomagune.es
Dr. S. Moreno-Flores, Dr. A. Kasry, Prof. Dr. H.-J. Butt, Dr. J. L. Toca-Herrera
Max-Planck-Institut für Polymerforschung
Ackermannweg 10, 55128 Mainz (Germany)
Dr. A. Kasry
Cardiff School of Biosciences
Biomedical Science Building
Museum Avenue, Cardiff CF103US (UK)
C. Vavilala, Prof. Dr. M. Schmittel
Organische Chemie I
Universität Siegen
Adolf-Reichwein-Strasse 3, 57068 Siegen (Germany)
Dr. D. Pum, Prof. Dr. U. B. Sleytr
Zentrum für Nanobiotechnologie
Universität für Bodenkultur
Gregor Mendel Strasse 33, 1180 Wien (Austria)

[**] S.M.-F. thanks the Max-Planck-Gesellschaft for financial support and acknowledges Rüdiger Berger and Prof. Wolfgang Knoll for the AFM&SPR facilities. J.L.T.-H. thanks the Ramón y Cajal program of the Spanish government. The authors are grateful to Jacqueline Friedmann for technical support on S-proteins and Kathryn Melzak, Radostina Georgieva, and Paula Pescador for useful comments. We are indebted to the Deutsche Forschungsgemeinschaft for support on the synthetic work. This work has been additionally supported by the US Air Force Office of Scientific Research (project nos.: FA9550-06-0208 and FA9550-07-1-0313) and the Spanish Government (grant no.: CTQ2007-66541).

Supporting information for this article is available on the WWW under http://www.angewandte.org or from the author.

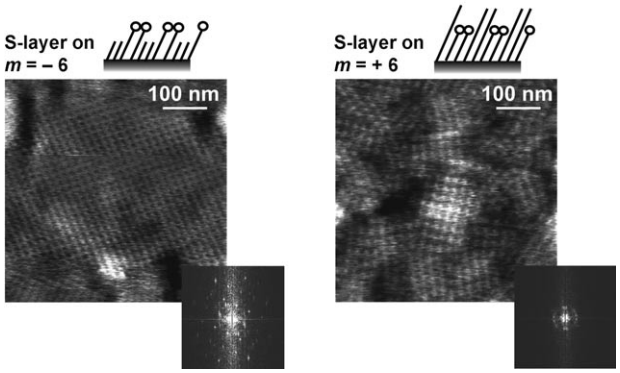

Figure 2. Contact-mode AFM height images of S-layers on disulfide SAMs with $m=-6$ and $m=+6$ (vertical scale: 3 nm). The insets show the corresponding 2D Fourier transformations from which the lattice parameters are extracted.

Table 1: Lattice parameters, crystal size, thickness, and recrystallization kinetics of S-layers recrystallized on disulfide SAMs with varying m values.

m	Lattice parameters		Crystal size [nm^2]	Thickness [nm]	Kinetics
	a [nm]	b [nm]			
−6	12.7±0.2	12.4±0.5	(1.3±0.1)×10^5	15.2±0.3	2 step
−4	13.7±0.2	13.4±0.3	(6.5±0.6)×10^4	14.1±0.2	2 step
−2	13.7±0.3	12.7±0.3	(6.7±0.5)×10^4	13.4±1.5	2 step
0	13.3±0.3	12.77±0.08	(4.7±0.5)×10^4	15.1±0.3	2 step
+2	14.0±0.5	13.0±0.8	(2.0±0.3)×10^4	9.6±0.4	2 step
+4	14.2±0.2	13.8±0.2	(8.2±0.8)×10^3	8.2±0.3	1 step
+6	15.6±0.5	15.2±0.4	(1.2±0.6)×10^4	8.6±0.2	1 step

circle). When $m=+6$, this shoulder does not appear and the curve increases uniformly before it reaches a stable value (Figure 3b and inset). AFM images obtained during crystallization show that, for $m=-6$, the process is characterized by an initial adsorption of a few nucleation points (Figure 3c) followed by growth (Figure 3d) and ultimate reorganization of the layer (Figure 3e), whereas, for $m=+6$, recrystallization proceeds through adsorption of numerous nucleation points (Figure 3f), which undergo no or very limited crystal growth (Figure 3g) until complete surface coverage (Figure 3h).

The S-protein used (SbpA CCM 2177) is anisotropic, with outer and inner sides.[2] The outer side is smooth, neutral, and exposed to the medium in bacteria. The inner side is more corrugated, negatively charged, and binds to the cell wall through lectin-mediated interactions. Apparently, only the inner side of the S-layer can act as a substrate for a second protein layer. In accordance with this, different scenarios for S-protein recrystallization on disulfide SAMs can be proposed (Figure 4).

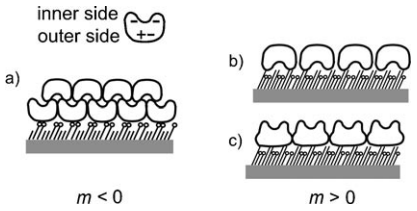

Figure 4. Different scenarios for S-protein adsorption on disulfide SAMs with varying m values: For $m=-6$, bilayers form (a); for $m=+6$, monolayers form upon adsorption either through the inner sides (b) or through the outer sides (most plausible; c).

In bilayers, the neutral side of the S-protein predominantly binds to the substrate and consequently the monolayers interact through their inner sides[11] (Figure 4a). For monolayers, the question to address is how the proteins adsorb. Assuming that proteins adsorb through either their outer or inner sides, we can evaluate both possibilities. Inner-side adsorption (Figure 4b) is energetically unfavorable due to the hydrophobic SAM. Additionally, if the outer side were exposed to the medium, the S-layer properties for bilayers and monolayers would be identical. Figure 5a shows force–distance curves for S-layers formed on SAMs with $m=+6$ and $m=-6$ in water; the difference between the curves reveals that the surface properties are different. The interactions between the AFM tip and the S-layer when $m=-6$ in water greatly resemble those observed on S-layers deposited on hydrophilic supports, such as silicon wafers,[10] polyelectrolytes,[11] or lipid layers.[14] On the other hand, the long-

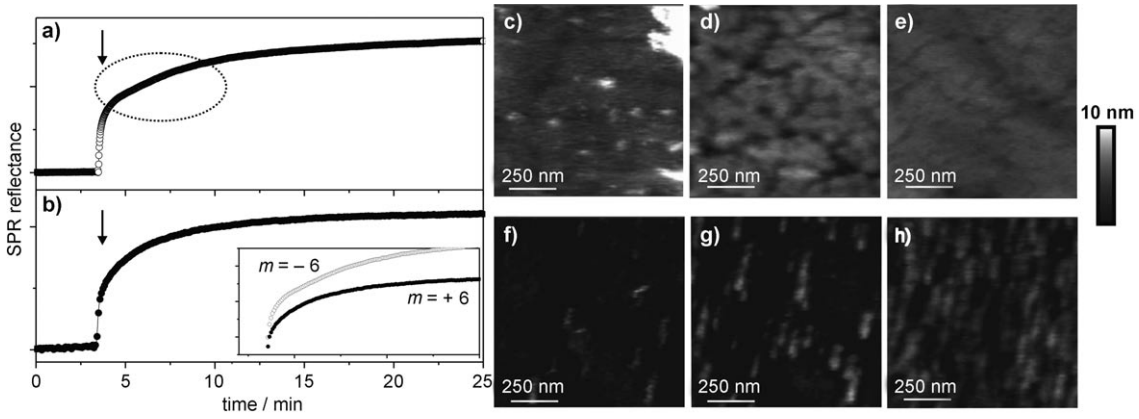

Figure 3. SPR reflectivity versus time for S-proteins recrystallizing on disulfide SAMs with $m=-6$ (a) and $m=+6$ (b). The inset shows both curves in the region of the dotted circle. The arrows indicate the time of injection of the protein solution. Sequential in situ AFM height images during protein recrystallization on disulfide SAMs with $m=-6$ (c–e) and with $m=+6$ (f–h).

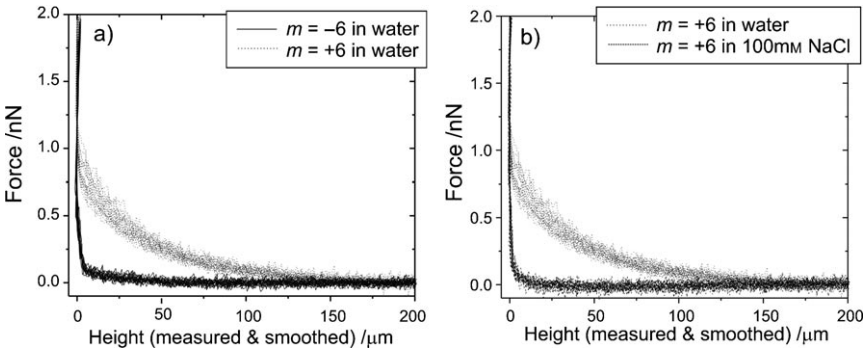

Figure 5. Force–distance (approach) curves between an AFM tip and S-layers formed on disulfide SAMs: a) with $m=-6$ and $m=+6$ in water; b) with $m=+6$ in water and with added salt (1:1). A total of 19–20 curves are shown for each system.

range repulsion observed when $m=+6$ is mainly of electrostatic nature, since it is screened out when electrolyte is added (100 mM NaCl, Figure 5b). The absence of this repulsion in $m=-6$ SAMs indicates that different protein sides are exposed in each case and, hence, the scenario depicted in Figure 4c is the most plausible when $m=-6$.

Such a disparity in both crystal morphology and crystal formation can only be due to the different end-group chemistry and the extent of the protruding groups. On SAMs with $m=+6$, the protein adsorption is mainly driven by hydrophobic interactions: AFM images of S-layers on hydrophobic SAMs have similar morphology (see the Supporting Information). In this case, monolayer formation is likely favored due to protein deformation upon adsorption.[15] For SAMs with $m=-6$, the protruding hydroxy-terminated chains predominantly interact with the proteins through H-bonds.[16] In this case, the use of disulfide SAMs particularly favors protein recrystallization by lowering the OH–surface ratio and enhancing end-group accessibility.

Herein, we have described the manipulation of S-layers by tuning substrate–protein interactions at the nanoscale. This has been achieved by using disulfide SAMs containing chemical end groups with different polarities. Monolayer protein crystals are formed when hydrophobic end groups protrude from the substrate. The square lattices have a periodicity of (15.5 ± 0.5) nm. In this case, hydrophobic interactions are responsible for protein adsorption without any or with very limited crystal growth and for expansion of the crystalline lattice. Bilayers of S-proteins are formed on protruding hydrophilic (hydroxy) groups. The S-layers are quasisquare lattices with a periodicity of (13 ± 1) nm, typical of native protein crystals. In this case, H-bonding results in protein adsorption followed by substantial crystal growth and protein rearrangement. The transition from non-native to native S-layers occurs upon elongation of the OH-terminated thiolates by at least four methylene units over the CH_3-terminated ones. The experimental findings constitute proof of terminal-group accessibility in disulfide SAMs for establishing interactions with biomacromolecules as well as the tremendous influence of end groups on non-ligand-mediated protein recrystallization, which opens the way to use these groups as templates for biomineralization.

Experimental Section

Sample preparation: The bacterial S-protein (SbpA) was isolated form *Bacillus sphaericus* CCM 2177. The extraction of the protein from the bacterial species was performed as described elsewhere,[19] and the extract was centrifuged (3500 rpm, 5 min) to remove protein aggregates. The protein solution used for recrystallization experiments was prepared by dilution of the supernatant of the protein extract at a ratio of 1:10 in 0.5 mM tris(hydroxymethyl)aminomethane/HCl buffer (pH 9) containing 10 mM $CaCl_2$. The final concentration of the protein monomers was ≤ 1 mg mL^{-1}.

The synthesis and preparation of the disulfide SAMs on gold substrates for AFM and SPR analysis were performed according to an already reported procedure.[7] The gold substrates for SPR experiments were prepared by thermal evaporation (50 ± 5 nm) onto LaSFN9 glass slides ($n=1.85$) previously coated with an adhesive layer of chromium (approximately 2 nm). Samples for ex situ AFM experiments were prepared on freshly prepared disulfide SAMs by overnight incubation of the samples (1×1 cm^2) in the protein-containing solution. Subsequently, the samples were rinsed in Milli-Q water and mounted in the AFM setup.

AFM measurements: All experiments were performed in contact mode in water or aqueous solutions of NaCl (0.1M) at room temperature, by using a multimode atomic force microscope and a Nanoscope IIIa controller (Veeco Instruments, Santa Barbara, CA) equipped with a 12×12 μm^2 scanner. Silicon nitride cantilevers with a nominal spring constant of 0.1 N m^{-1} (NP, NP-S, Veeco Instruments) were used for imaging the recrystallized S-proteins. The scanning force was adjusted to be below 0.5 nN to minimize tip-induced damage of the sample. Force–distance curves were obtained as follows: the AFM tip was repeatedly brought into contact with the S-layer and withdrawn at a speed of 500 nm s^{-1}. The cantilever deflection was monitored as a function of the extension of the piezoscanner and converted into force units by using the cantilever spring constant. The tip–sample separation was calculated by subtracting the cantilever deflection from the piezoscanner displacement. Maximum compressive loads did not exceed 10 nN.

SPR measurements: A homemade setup based on the Kretschmann configuration[20] with an LaSFN9 prism was used. The incident light source was a He–Ne laser ($\lambda=632.8$ nm); reflected light was measured with a photodiode. Reflectivity curves were measured in buffer as a function of the incident angle in order to determine the resonance angle at which the reflectivity is at minimum. The time evolution of the reflectivity signal at a fixed angle was used to follow the adsorption kinetics after protein injection. This angle was set slightly smaller than the resonance angle to enhance instrumental sensitivity. Rinsing of the surfaces after completion of recrystallization did not induce desorption.

Received: January 11, 2008
Revised: March 25, 2008
Published online: May 16, 2008

Keywords: adsorption · crystal engineering · proteins · protein–substrate interactions · self-assembled monolayers

[1] N. E. Chayen, *Curr. Opin. Struct. Biol.* **2004**, *14*, 577–583.
[2] U. B. Sleytr, M. Sara, D. Pum, B. Schuster, *Prog. Surf. Sci.* **2001**, *68*, 231–278.

[3] C. Huber, J. Lui, E. M. Egelseer, D. Moll, W. Knoll, U. B. Sleytr, M. Sára, *Small* **2006**, *2*, 142 – 150.
[4] U. B. Sleytr, N. Ilk, E. M. Egelseer, D. Pum, B. Schuster, *FEBS J.* **2007**, *274*, 323 – 334.
[5] W. Frey, W. R. Schief, Jr., D. W. Pack, C.-T. Chen, A. Chilkoti, P. Stayton, V. Vogel, F. H. Arnold, *Proc. Natl. Acad. Sci. USA* **1996**, *93*, 4937 – 4941.
[6] a) S. A. Darst, H. O. Ribi, D. W. Pierce, R. D. Kornberg, *J. Mol. Biol.* **1988**, *203*, 269 – 273; b) E. E. Uzgiris, R. D. Kornberg, *Nature* **1983**, *301*, 125 – 129.
[7] U. B. Sleytr, P. Messner, D. Pum, M. Sára, *Angew. Chem.* **1999**, *111*, 1098 – 1120; *Angew. Chem. Int. Ed.* **1999**, *38*, 1034 – 1054.
[8] H. Engelhardt, J. Peters, *J. Struct. Biol.* **1998**, *124*, 276 – 302.
[9] S. Moreno-Flores, A. Shaporenko, C. Vavilala, H.-J. Butt, M. Schmittel, M. Zharnikov, R. Berger, *Surf. Sci.* **2006**, *600*, 2847 – 2856.
[10] E. Györvary, O. Stein, D. Pum, U. B. Sleytr, *J. Microsc.* **2003**, *212*, 300 – 306.
[11] J. L. Toca-Herrera, R. Krastev, V. Bosio, S. Küpcü, D. Pum, A. Fery, M. Sára, U. B. Sleytr, *Small* **2005**, *1*, 339 – 348.
[12] M. Weygand, B. Wetzer, D. Pum, U. B. Sleytr, N. Cuvillier, K. Kjaer, P. B. Howes, M. Loesche, *Biophys. J.* **1999**, *76*, 458 – 468.
[13] D. Pum, U. B. Sleytr, *Colloids Surf. A* **1995**, *102*, 99 – 104.
[14] Y. F. Dufrêne, *Micron* **2001**, *32*, 153 – 165.
[15] a) S. Cheng, K. Chittur, C. Sukenik, L. Culp, K. Lewandowska, *J. Colloid Interface Sci.* **1994**, *162*, 135 – 143; b) P. Roach, D. Farrar, C. C. J. Perry, *J. Am. Chem. Soc.* **2005**, *127*, 8168 – 8173.
[16] Electrostatic forces between deprotonated OH groups (denoting acid behavior) and positive rests of protein amino acids are ruled out in a first approximation. Titration curves obtained by scanning force microscopy with chemically modified tips[17] have demonstrated that OH-terminated SAMs do not exhibit pH dependence throughout the pH range considered (pH 2–12), in contrast to what was observed on amino- and carboxy-terminated SAMs.[17,18] Since S-protein recrystallization was performed at pH 9, we infer that our SAMs do not exhibit acid behavior under these conditions.
[17] E. W. van der Vegte, G. Hadziioannou, *Langmuir* **1997**, *13*, 4357 – 4368.
[18] a) K. Hu, A. J. Bard, *Langmuir* **1997**, *13*, 5114 – 5119; b) T. R. Lee, R. I. Carey, H. A. Biebuyck, G. M. Whitesides, *Langmuir* **1994**, *10*, 741 – 749.
[19] U. B. Sleytr, M. Sára, S. Küpcü, P. Messner, *Arch. Microbiol.* **1986**, *146*, 19 – 24.
[20] E. Kretschmann, H. Raether, *Z. Naturforsch. A* **1968**, *23*, 2135 – 2136.

